THE JOURNAL OF BIOLOGICAL CHEMISTRY

Vol. 268, No. 19, Issue of July 5, pp. 14081-14089, 1993
Printed in U.S.A.

Conformations of Peptide Fragments Comprising the Amino-terminal, Central, and Carboxyl-terminal Regions of a Membrane-active Polypeptide

BUILD-UP OF SECONDARY STRUCTURE IN PARDAXIN*

(Received for publication, January 22, 1993, and in revised form, March 17, 1993)

Gayatri Saberwal‡ and Ramakrishnan Nagaraj§

From the Centre for Cellular and Molecular Biology, Uppal Road, Hyderabad 500 007, India

The conformations of synthetic peptides of different lengths corresponding to the amino-terminal, central, and carboxyl-terminal regions of pardaxin (GFFALIPKIISSPLFKTLLSAVGSALSSSGEQE) have been studied by circular dichroism spectroscopy. The peptides GFFALIPKIISSPLF-OMe, GFFALIPKIISSPLFK-OMe corresponding to the amino-terminal region, as well as peptides KIISSPLFKTLLSAV and IISSPLFKTLLSAV corresponding to the central region of the toxin have a marked tendency to adopt helical conformation. Ordered conformation is also discernible in the 8- and 7-residue peptides GFFALIPK-OMe and IISSPLF-OMe. Peptides corresponding to the central segments KTLLSAV, LSAVGSAL, and the carboxyl-terminal segment SSSGEQE, however, exhibit very little secondary structure. The peptide segments that adopt ordered conformation show similar conformation when present in the entire toxin as suggested by proton magnetic resonance data (Zagorski, M. G., Norman, D. G., Barrow, C. J., Iwashita, T., Tachibana, K., and Patel, D. J. (1991) *Biochemistry* 30, 8009–8017). The observation that peptide segments corresponding to the amino-terminal and central regions of the toxin adopt ordered conformations compared to the carboxyl-terminal segment in isolation as well as in the toxin, indicates a role for these regions in initiating and maintaining ordered conformation of pardaxin.

Pardaxin is a 33-residue peptide toxin present in the defense secretions of certain species of soles of the genus *Pardachirus* (Primor and Zlotkin, 1976). The toxin has attracted attention due to its shark-repelling properties (Primor *et al.*, 1978) as well as its ability to exhibit diverse pathological and pharmacological effects (Primor and Tu, 1980; Primor *et al.*, 1980, 1983; 1984; Primor and Lazarovici, 1981; Primor, 1984; Pal *et al.*, 1981; Primor and Zlotkin, 1975). The biological activities of pardaxin are presumed to arise from its ability to perturb membranes. Support for this assumption comes from the observation that the peptide is highly surface-active and interacts with model membranes of phosphatidylcholine and serine (Lelkes and Lazarovici, 1988). However, pardaxin does not have any primary structural similarity with other toxins. In order to identify potential folding initiation sites in proteins, conformational preferences of synthetic peptides spanning the entire length of the polypeptide chain have been examined (Dyson *et al.*, 1992). A good correlation was observed between the helical regions of the four-helix bundle protein myohemerythrin and the conformational properties of peptides corresponding to these regions. Thus, conformational propensities of short peptide segments are likely to have a role in the initiation of folding in proteins. There have been reports on the structural studies of short peptide toxins (Zagorski *et al.*, 1991; Nagaraj and Balaram, 1981a, 1981b, 1981c; Fox and Richards, 1982; Dempsey, 1990; Lee *et al.*, 1987). However, the role of various regions in dictating the conformation of the entire toxin is not clear except in the case of alamethicin. In this 20-residue peptide, the dialkyl amino acid α-aminoisobutyric acid forces a helical conformation (Nagaraj *et al.*, 1979; Nagaraj and Balaram, 1981a, 1981b, 1981c) as the allowed conformational space for this amino acid in the Ramachandran map (Ramachandran and Sasisekharan, 1968) is restricted to the helical region only. Hence, it would be pertinent to examine the conformational propensities of peptides corresponding to different segments of peptide toxins. Such analysis would also aid in the rational design of hybrid toxins (Boman *et al.*, 1989; Andreu *et al.*, 1992) which are composed of sequences from different peptide toxins. Structure-function studies on "hybrid toxins" are of considerable interest as some of them appear to have specific biological activity like only antibacterial activity (Boman *et al.*, 1989; Andreu *et al.*, 1992).

The primary structure of pardaxin (Thompson *et al.*, 1986) (Table I) reveals a 26-residue apolar stretch beginning from the amino terminus followed by a polar and charged 7-residue carboxyl-terminal fragment. It has been demonstrated that the amino-terminal tetrapeptide GFFA is essential for toxin action (Lelkes and Lazarovici, 1988). Also, an analog that lacks the carboxyl-terminal polar heptapeptide has a 4000-fold decreased channel-forming ability (Lelkes and Lazarovici, 1988). Thus, both ends of the toxin appear to be important for toxin action. Based on the membrane-perturbing abilities of several analogs, it has been proposed that residues 2–10 form an α-helix and are involved in the insertion of the peptide within the bilayer and aggregation, whereas residues 13–27 form the putative ion channel lining segment (Shai *et al.*, 1990). We have shown that a peptide corresponding to residues 1–15 of pardaxin perturbs model membranes (Saberwal and Nagaraj, 1989), suggesting a role for the amino-terminal region other than solely being involved in promoting aggregation. Based on a recent nuclear magnetic resonance (NMR) study (Zagorski *et al.*, 1991), it has been suggested that peptide segments 7–11 and 14–26 are helical, while

* The costs of publication of this article were defrayed in part by the payment of page charges. This article must therefore be hereby marked "*advertisement*" in accordance with 18 U.S.C. Section 1734 solely to indicate this fact.

‡ Present address: Dept. of Physiology & Biophysics, Cornell University Medical College, New York, NY 10021.

§ To whom correspondence and reprint requests should be addressed.

TABLE I
Sequences of pardaxin and synthetic peptides corresponding to its different segments

GFFALIPKIISSPLFKTLLSAVGSALSSSGEQE
GFFALIPK-OMe
IISSPLF-OMe
G F F A L I P K I I S S P L F-OMe (15P-OMe)
G F F A L I P K I I S S P L F K-OMe (16P-OMe)
K T L L S A V-OMe
L S A V G S A L-OMe
K T L L S A V G S A L-OMe (11P-OMe)
I I S S P L F K T L L S A V (14P)
Acetyl-K I I S S P L F K T L L S A V (AcK15P)
S S S G E Q E-OMe

residues at the amino and carboxyl terminus exist predominantly in *extended* conformations. In an effort to determine the role of various regions of pardaxin in initiating and directing secondary structure, conformational analysis of synthetic peptides corresponding to amino-terminal, central, and carboxyl-terminal regions of the toxin by circular dichroism (CD) spectroscopy was undertaken, and the results are described in this paper.

EXPERIMENTAL PROCEDURES

Synthesis of Peptides—Peptides listed in Table I were synthesized by solid-phase and solution-phase methods. In solution-phase synthesis, dipeptide couplings were effected in dichloromethane (CH_2Cl_2) by dicyclohexylcarbodiimide. Tripeptides and longer peptides were synthesized in dimethylformamide with dicyclohexylcarbodiimide and 1-hydroxybenzotriazole. In solid-phase synthesis, the peptide chain was built on a Merrifield resin using *t*-butyloxycarbonyl chemistry, manually. The protocols employed were essentially as described for signal sequences (Reddy *et al.*, 1985; Reddy and Nagaraj, 1986, 1989) and hydrophobic peptides like alamethicin (Nagaraj and Balaram, 1981a, 1981b, 1981c). All protected peptides were purified by column chromatography on silica gel (230–400 mesh, Merck, Germany) using mixtures of chloroform and methanol as eluants. The deprotected peptides 15P-OMe, Ac14P, and AcK15P were purified using fast performance liquid chromatography (FPLC),[1] using an analytical pepRPC (reverse phase, C18) column. The homogeneity of all peptides was confirmed by FPLC under similar conditions and quantitative amino acid analysis done on an LKB 4151 alpha plus amino acid analyzer. Details of the amino acid analysis are summarized in Table II.

Circular Dichroism (CD) Studies—Spectra were obtained on the JASCO J-20 spectrometer and Jobin-Yvon Dichrograph V. The spectrometers were calibrated with (+)-10-camphorsulfonic acid. Cells of 0.1-cm path length were used, and the spectra were run at the ambient temperature of 22 °C. θ values correspond to mean residue ellipticities.

Preparation of Peptide Samples for CD—All peptide stock solutions were made up in MeOH. These stocks were subjected to quantitative amino acid analysis. Aliquots of peptide stock solution were transferred to acid-washed test tubes (3 ml) and dried using the Savant Speed-Vac. Appropriate spectroscopic grade solvent (hexafluoroisopropanol, methanol, or trifluoroethanol) was added to make up to a known concentration just before recording the spectrum. For studies with SDS micelles, the peptide stock aliquots were transferred to tubes that were then subjected to Savant Speed-Vac drying. Appropriate volumes and concentrations (above the critical micelle concentration of 8 mM) of SDS solution was then added prior to running the sample. All spectra were baseline-corrected. The CD spectra of the 14–16-residue peptides were analyzed for helical content according to the method of Taylor and Kaiser (Taylor and Kaiser, 1987). This method compares the experimental ellipticity at 222 nm to a theoretical value and has been routinely used to estimate helical structures in signal sequences and model peptides (Bruch and Gierasch, 1990; Padmanabhan *et al.*, 1990; Hoyt and Gierasch, 1991; Keller *et al.*, 1992).

[1] The abbreviations used are: FPLC, fast protein liquid chromatography; HFIP, hexafluoroisopropanol; OMe, methyl ester; TFE, trifluoroethanol.

RESULTS

Amino-terminal Fragments

15P-OMe—The spectra in TFE, SDS micelles, and lysophosphatidylcholine micelles are shown in Fig. 1. All spectra show two minima ~208 nm and 220 nm with a crossover of ~200 nm. The spectra are characteristic of peptides in the α-helical conformation. Estimation of helix content yields a value of 32% in TFE and 27% in SDS. In HFIP and MeOH (Fig. 2), the intensity of the 200 nm band is greater than the 220 nm band. The crossover is also at a lower wavelength. Thus, in HFIP and MeOH, there is a decrease in helix content and an increase in random structure.

16P-OMe—The spectra of this peptide in TFE and SDS micelles are shown in Fig. 3. The intensities of the 207 and 222 nm bands are comparable. The spectra indicate that the peptide adopts helical conformation. Estimation of helical content yields 42% in TFE and 35% in SDS. Length-dependent estimates of Chen and co-workers (Chen *et al.*, 1974) also fall in the same range. 16P-OMe is 15P-OMe with a carboxyl-terminal extension of lysine. The extra lysine appears to have caused a slight increase in helical content.

GFFALIPK-OMe—The spectra of this peptide in HFIP, MeOH, TFE, and SDS micelles are as in Fig. 4. The ~220 nm (+)ve band could arise due to β-turn conformation adopted by the peptide and also due to interaction of the aromatic Phe with the backbone peptide group. The TFE spectrum has a strong (−)ve band at 205 nm and a weaker ~230 nm (−)ve band. The ~230 nm (−)ve band along with the ~205 nm (−)ve band could reflect a Type I turn of the Class C type of turn spectra. The peptide is clearly more ordered in SDS than in other solvents. The spectrum suggests a β-turn conformation for the peptide in SDS rather than other ordered structures like an α-helix or β-sheet.

IISSPLF-OMe—The spectra in various solvents are shown in Fig. 5. All the spectra show negative bands in the regions of wavelength that are characteristic of an α-helix, *i.e.* ~205 nm (−) and ~225 nm (−). The crossover in the MeOH and TFE spectra is ~197 nm, which is close to 200 nm, characteristic for peptides having a high α-helical content. Since a single phenylalanine can give rise to the aromatic ~220 nm (+) band, it is possible that the reduced intensity of the ~220 nm band is partly due to the aromatic contribution. Other 6–7-residue homo-oligo peptides have also been shown to adopt helical structure (Toniolo *et al.*, 1979). Thus, peptides corresponding to the amino-terminal segment of pardaxin clearly have a strong tendency to adopt α-helical conformation, particularly in the hydrophobic environment.

Central Fragments

14P—The spectra of this peptide in TFE and SDS micelles are shown in Fig. 6. Going by the relative intensities of the ~207 nm and ~222 nm bands, and crossover at ~200 nm, the spectra of this peptide are indicative of an exclusively α-helical secondary structure with no β-sheet structure. Analysis of the spectra indicates 44% α-helix in TFE and SDS. The spectra of amino-terminal acetylated 14P and 14P-$CONH_2$ were very similar to that of 14P indicating that the peptide does not undergo any major structural change with different amino- and carboxyl-terminal protecting groups.

AcK15P—The spectra of this peptide in TFE and SDS micelles are as in Fig. 7. This peptide comprises 14P extended at the amino terminus by a lysine. Here too, the relative intensities of the ~207 and ~222 nm bands and the ~200 nm crossover are indicative of a helical conformation. The ~207 nm band of the TFE spectrum is more intense than the ~220

TABLE II

Amino acid analysis of synthetic peptides corresponding to various segments of paradaxin

Theoretical values are in parentheses. S/T values not corrected for loss during hydrolysis.

Peptide	A	E	G	I	L	K	F	P	S	T	V
GFFALIPK-OMe	1.08		1.01	0.89	0.96	1.0	2.0	0.97			
	(1.0)		(1.0)	(1.0)	(1.0)	(1.0)	(2.0)	(1.0)			
IISSPLF-OMe				1.7	1.0		1.0	0.9	1.57		
				(2.0)	(1.0)		(1.0)	(1.0)	(2.0)		
15P-OMe	0.95		1.18	2.75	2.02	0.91	2.79	2.0	1.34		
	(1.0)		(1.0)	(3.0)	(2.0)	(1.0)	(3.0)	(2.0)	(2.0)		
KTLLSAV-OMe	1.0				2.10	1.0			0.9	0.9	0.9
	(1.0)				(2.0)	(1.0)			(1.0)	(1.0)	(1.0)
LSAVGSAL-OMe	2.0		0.82		2.0				0.92		1.23
	(2.0)		(1.0)		(2.0)				(2.0)		(1.0)
11P-OMe	2.18		0.94		3.24	0.94			1.0	0.55	1.0
	(2.0)		(1.0)		(3.0)	(1.0)			(2.0)	(1.0)	(1.0)
14P	1.02			1.29	2.97	0.9	0.95	0.91	1.57	0.63	1.11
	(1.0)			(2.0)	(3.0)	(1.0)	(1.0)	(1.0)	(3.0)	(1.0)	(1.0)
AcK15P	0.96			1.38	3.13	2.0	1.11	0.99	1.94	0.90	1.05
	(1.0)			(2.0)	(3.0)	(2.0)	(1.0)	(1.0)	(3.0)	(1.0)	(1.0)
SSSGEQE-OMe		3.08	1.0						2.63		
		(3.0)	(1.0)						(3.0)		

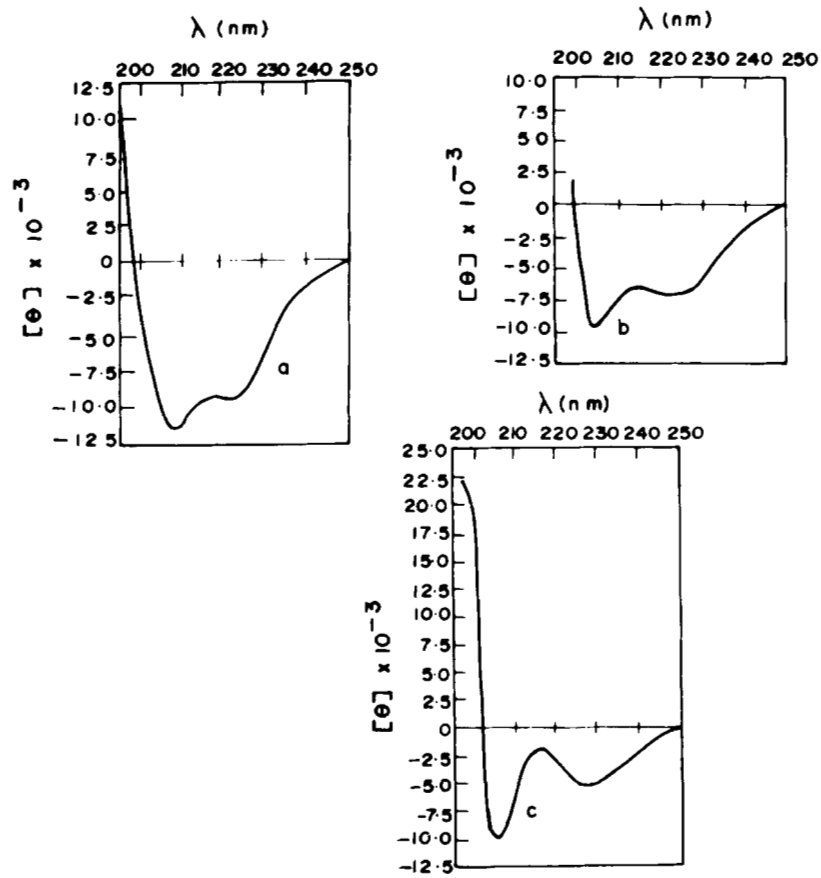

FIG. 1. **Spectra of 15P-OMe.** *a*, TFE (0.1 mg/ml); *b*, SDS micelles (0.1 mg/ml); *c*, lysophosphatidylcholine micelles (0.1 mg/ml).

nm band. The ~222 nm band intensity in either case is similar and corresponds to a high α-helical content of 67%. In contrast to the case of 15P-OMe and 16P-OMe, an extra lysine residue leads to a significant increase in percent helicity on going from 14P to AcK15P.

KTLLSAV-OMe—The spectra are shown in Fig. 8 and indicate that the peptide is unordered in all three organic solvents HFIP, MeOH, and TFE. The TFE spectrum has weak positive ~220 nm and ~240 nm bands and a negative band at ~200 nm. Likewise, the SDS spectrum has a prominent minimum ~200 nm and a shoulder at ~225 nm. This would argue against the peptide adopting a strongly helical structure in this medium. It is, however, possible that the spectrum is indicative of β-turn formation, although the ~200 nm (−) band is weak compared to that exhibited by an ideal β-turn. Thus, the spectrum suggests a mixture of β-turn and random conformation for the peptide in SDS.

LSAVGSAL-OMe—The spectra in different solvent systems are shown in Fig. 9. These spectra are also characteristic of the unordered conformation. However, the spectrum in TFE suggests that a small fraction of the peptide exists in a β-turn conformation.

11P-OMe—The spectra are shown in Fig. 10. In MeOH and HFIP, the spectra indicate that the peptide is unordered. On going to TFE, the peptide has a tendency to adopt a helical structure. However, the low $[\theta]_{222}$ value indicates only a small

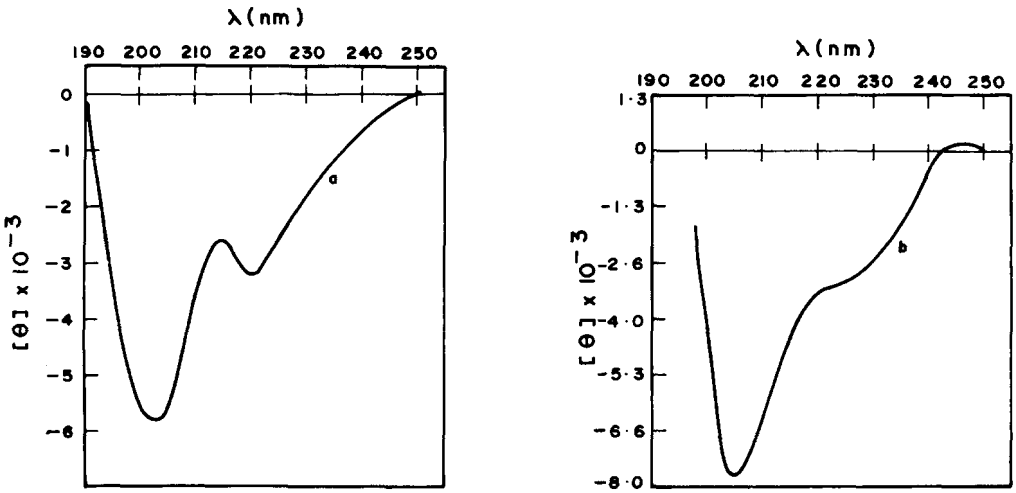

FIG. 2. **Spectra of 15P-OMe.** *a*, HFIP (0.1 mg/ml); *b*, MeOH (0.1 mg/ml).

FIG. 3. **Spectra of 16P-OMe.** *a*, 16P-OMe in TFE (0.07 mg/ml); *b*, 16P-OMe in SDS (0.07 mg/ml).

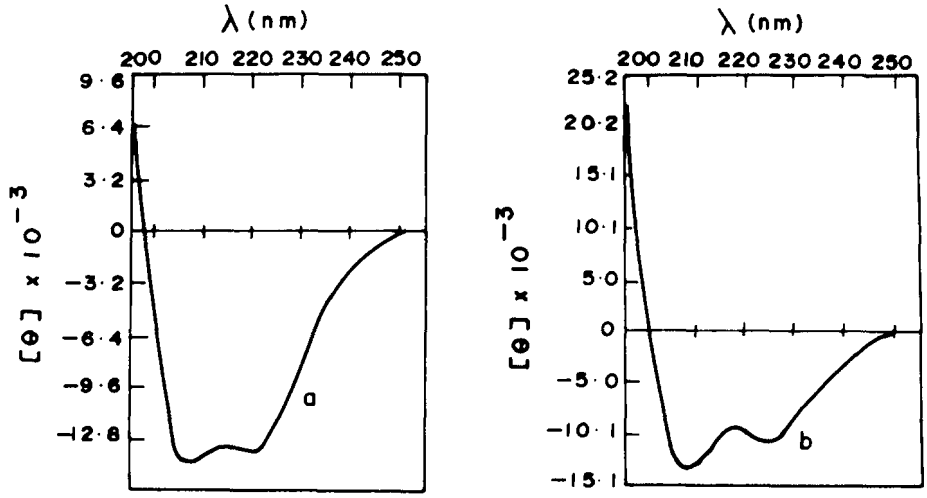

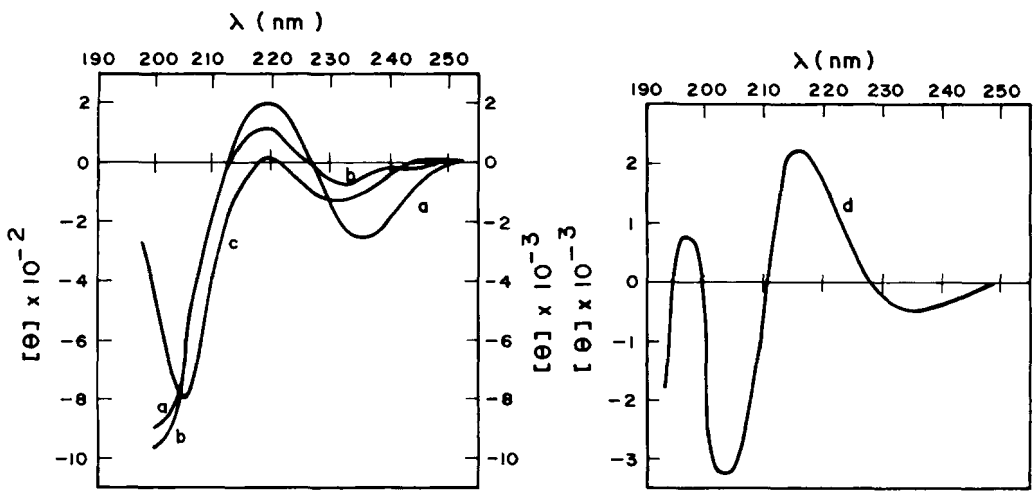

FIG. 4. **Spectra of GFFALIPK-OMe.** *a*, MeOH (0.58 mg/ml); *b*, HFIP (1.28 mg/ml); *c*, TFE (0.25 mg/ml) in units of $[\theta] \times 10^{-3}$; *d*, SDS micelles (0.5 mg/ml).

amount of helical structure, with the peptide largely adopting an unordered conformation. In SDS micelles, the spectrum has a more intense ~208 nm (−) band and an ~222 nm (−) shoulder, indicating higher helical content. Thus, 11P-OMe shows a marked tendency to adopt an α-helical conformation in media of increased hydrophobicity.

Carboxyl-terminal Segment: SSSGEQE-OMe

The spectra of this peptide have been obtained in HFIP, MeOH, TFE, and SDS micelles and are described in Fig. 11. The spectra in all solvent systems are archetypical "random" spectra, with a very weak ~230 nm (−) band and much stronger ~200 nm (−) band. The ~215 nm band may be

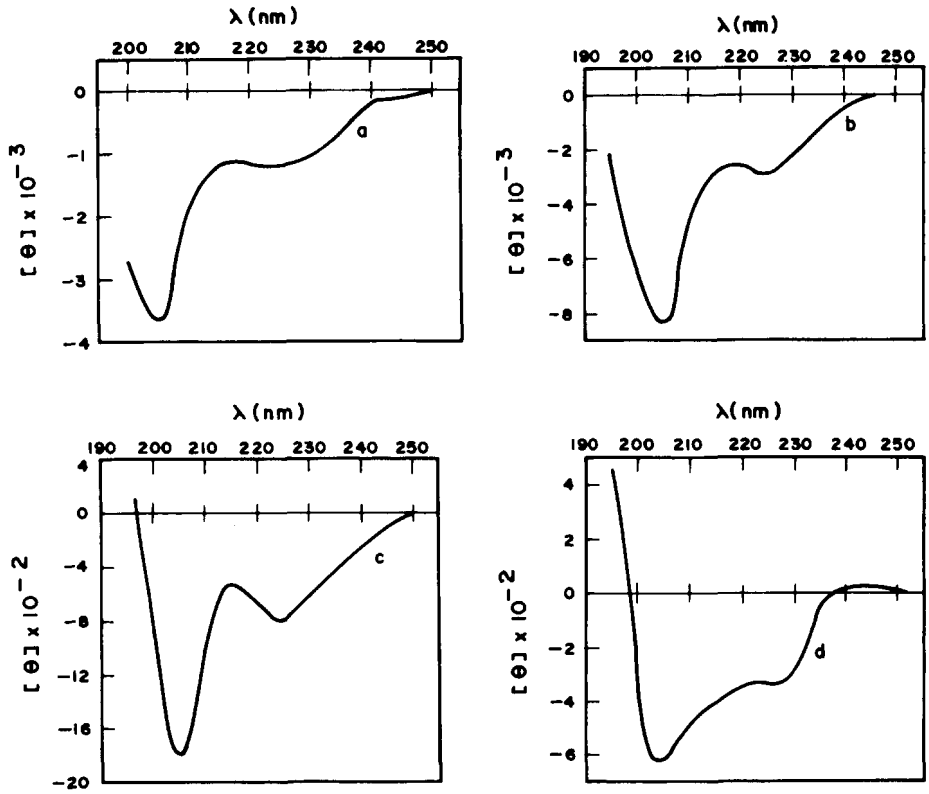

FIG. 5. **Spectra of IISSPLF-OMe.** *a*, SDS micelles (0.2 mg/ml); *b*, HFIP (0.1 mg/ml); *c*, MeOH (0.4 mg/ml); *d*, TFE (0.48 mg/ml).

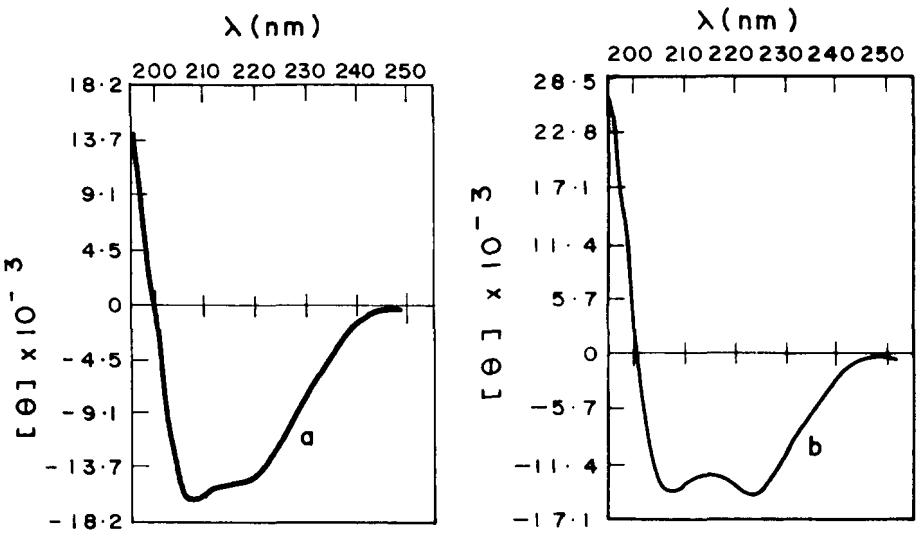

FIG. 6. **Spectra of 14P.** *a*, TFE (0.1 mg/ml); *b*, SDS (0.07 mg/ml).

negative or positive, as has been observed with other spectra indicative of unordered conformation (Mattice and Harrison, 1975).

The CD spectra of 15P-OMe, 16P-OMe, 14P, and AcK15P were independent of peptide concentration in the range of 0.05 mg/ml to 0.2 mg/ml. The shorter peptides also did not show any concentration dependence.

DISCUSSION

An α-helical conformation appears to be a common structural motif in a large number of peptide toxins comprising 13–35 residues (Kaiser and Kezdy, 1987). The Pardaxin sequence is composed of amino acids which can occur in helical and β-sheet conformations. Analysis of Pardaxin's primary sequence by the method of Chou and Fasman (Chou and Fasman, 1978) predicts 60% β-sheet, 20% α-helix, and 15% random coil, as shown below.

Primary sequence: GFFALIPKIISSPLFKTLLSAVGSALSSSGEQE; secondary structure prediction: *XXXX*BBBT BBBBBBBBBBBBBBBCCCCC*XXX*. (Notations are: *X*, helix; B, β-sheet; T, β-turn; C, random coil.)

The appearance of the CD spectra of pardaxin in MeOH and in the presence of lipid vesicles as well as the mean residue ellipticity values in the 217–222 nm region (Shai *et al.*, 1990) would suggest the presence of β-structure although it has been argued that the toxin adopts predominantly helical structure. Hence, a detailed study of the conformation of synthetic peptides corresponding to amino-terminal, central, and carboxyl-terminal regions of the toxin has been carried out in order to determine the importance of various segments of the toxin in initiating and maintaining ordered conformation.

The amino-terminal 15P-OMe and 16P-OMe exhibit α-

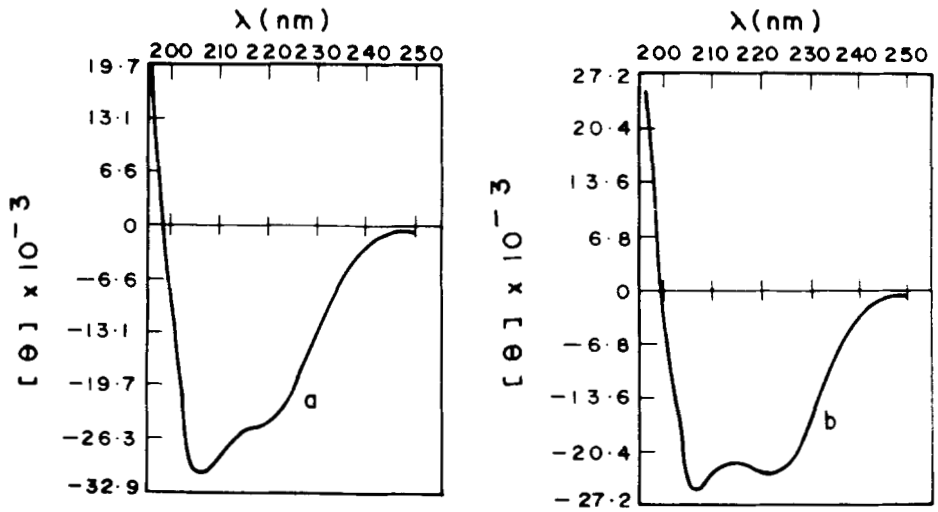

FIG. 7. **Spectra of AcK15P.** *a*, TFE (0.1 mg/ml); *b*, SDS (0.05 mg/ml).

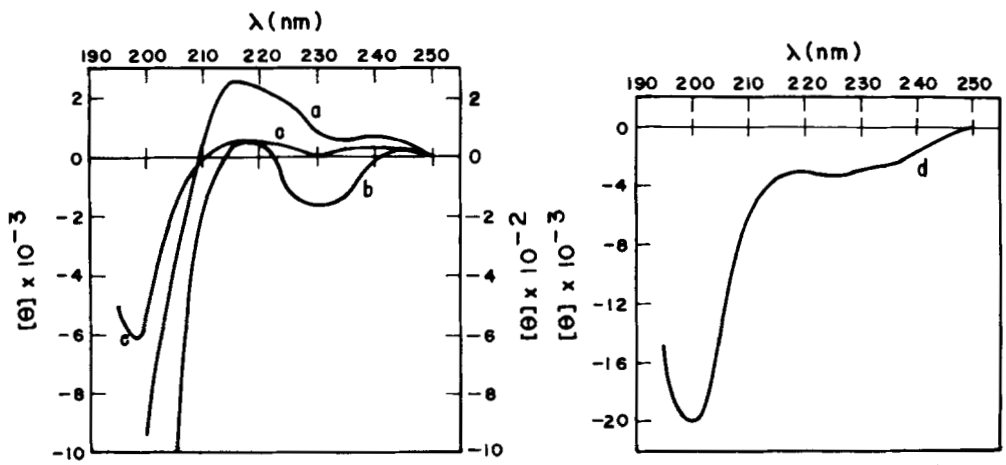

FIG. 8. **Spectra of KTLLSAV-OMe.** *a*, MeOH (0.35 mg/ml); *b*, HFIP (0.63 mg/ml), in units of $[\theta] \times 10^{-2}$; *c*, TFE (0.62 mg/ml); *d*, SDS micelles (0.2 mg/ml).

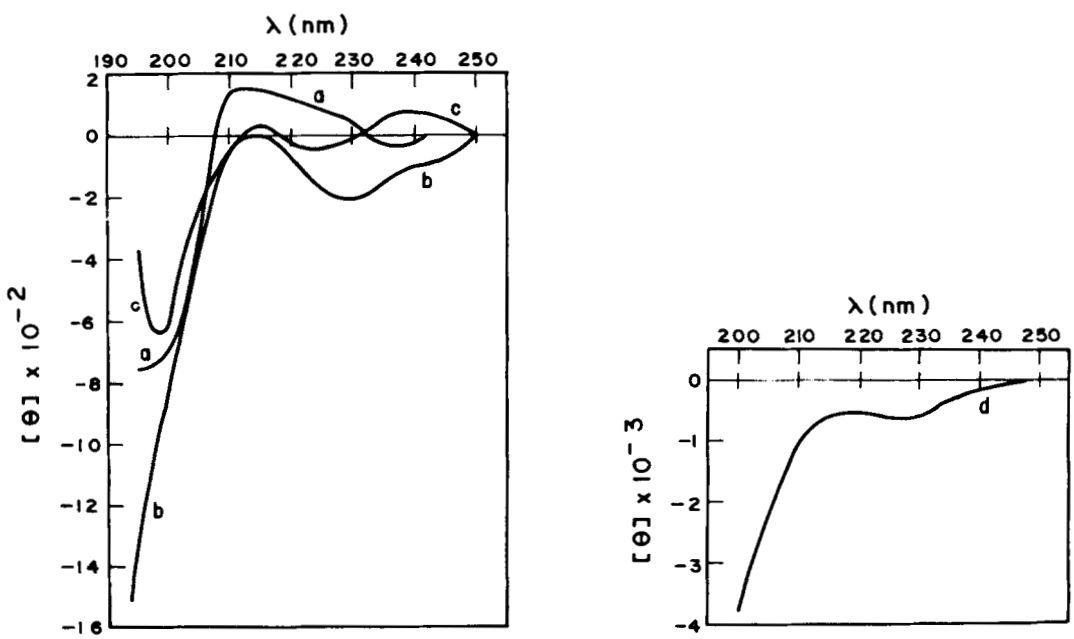

FIG. 9. **Spectra of LSAVGSAL-0Me.** *a*, MeOH (0.5 mg/ml); *b*, HFIP (0.33 mg/ml); *c*, TFE (0.5 mg/ml); *d*, SDS micelles (0.3 mg/ml).

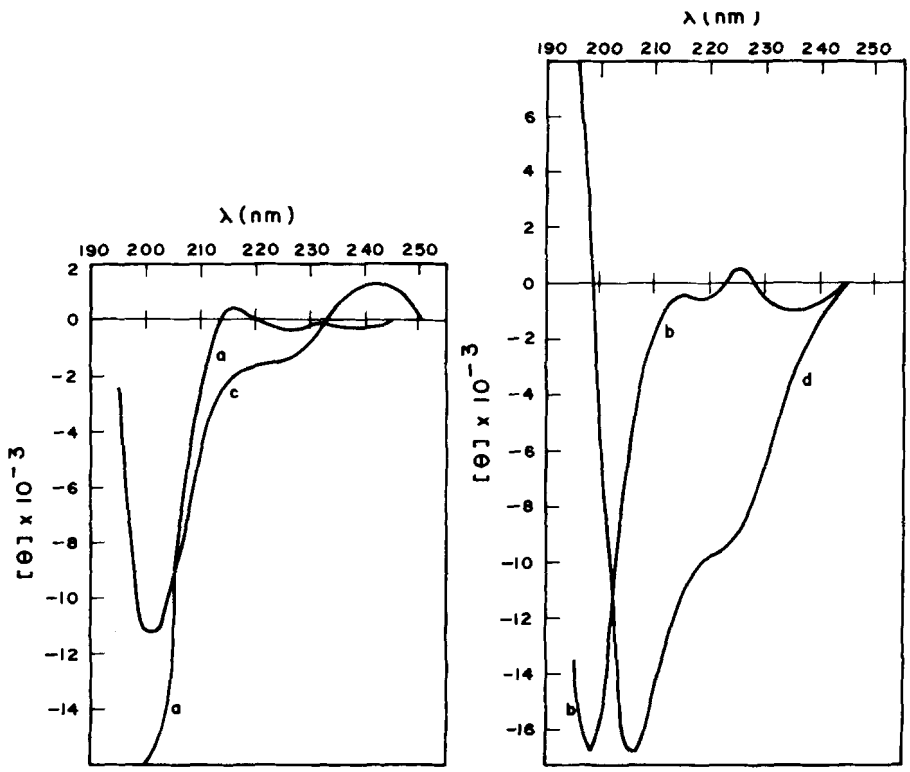

FIG. 10. **Spectra of 11P-OMe.** *a*, MeOH (0.15 mg/ml); *b*, HFIP (0.15 mg/ml); *c*, TFE (0.15 mg/ml); *d*, SDS micelles (0.15 mg/ml).

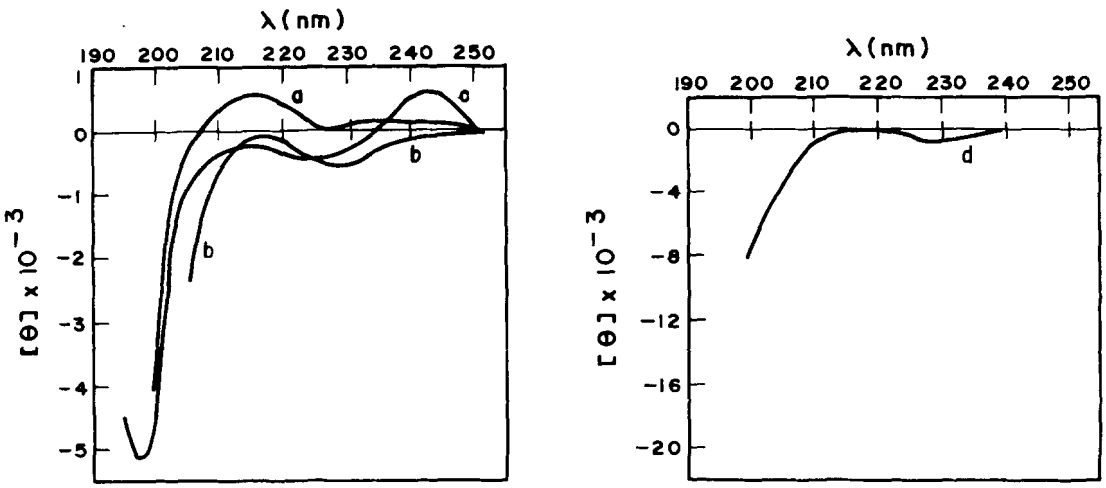

FIG. 11. **Spectra of SSSGEQE-OMe.** *a*, MeOH (0.8 mg/ml); *b*, HFIP (0.44 mg/ml); *c*, TFE (0.64 mg/ml); *d*, SDS micelles (0.5 mg/ml).

helix-type spectra in TFE and SDS, with crossovers at ~197–200 nm. The low intensity of the 207 nm and 222 nm bands indicate only ~25% helix, or alternately that the peptide is completely helical 25% of the time. Manning *et al.* (1988) have suggested that distortions of helical structure result in lower helical estimates due to a decrease in strength of the $n\pi^*$ transition and consequently result in the decrease in negative ellipticity at 222 nm. Also, the value of the negative ellipticity at 222 nm depends to a large extent on the length of the helix as well distortion in the helical structure (Manning *et al.*, 1988). For example, an 11-residue helical peptide could have a $[\theta]_{222}$ of −10,000 as compared to a value of −30,000 for an infinite helix. A good crossover for 15P-OMe and 16P-OMe in spite of $[\theta]_{222}$ of ~10,000 strongly argues for an ordered conformation. The 8- and 7-residue peptides GFFALIPK-OMe and IISSPLF-OMe also have a tendency to adopt ordered structures, particularly in a hydrophobic environment.

The central fragments KTLLSAV-OMe and LSAVGSAL-OMe exhibit very little secondary structure although 11P-OMe has a capacity to adopt helical structure in hydrophobic environments. Thus, this relatively less hydrophobic central fragment exhibits weak secondary structural propensities in isolation. Its carboxyl-terminal neighboring sequence, SSSGEQE, does not adopt any secondary structure, and, thus, its continuation in the carboxyl-terminal direction as 18P (KTLLSAVGSALSSSGEQE) does not bring about change in the secondary structure of this segment.[2] The amino-terminal IISSPLF-OMe, in contrast, does have a tendency to adopt helical structure, and it is likely that significant secondary structure may be induced in a longer peptide incorporating this peptide and 11P.

The central part of the toxin encompasses the sequences 14P and AcK15P. AcK15P is markedly more helical than 14P.

[2] S. Thennarasu and R. Nagaraj, unpublished data.

Thus, the amino-terminal lysine exerts a strong structure-promoting influence on this peptide, and the peptide is largely helical in spite of a proline in the middle of the sequence. Whereas 15P-OMe and 16P-OMe have 2 prolines each, 14P and AcK15P have only 1 proline each. The proline residues can bring about distortions in a helical structure and thereby cause a decrease in the $[\theta]_{222}$ value, especially in 14P and 15P-OMe, the shorter of the two pairs. In all four peptides, 1 proline occurs in the middle of the sequence. The second proline in 15P-OMe and 16P-OMe is the 3rd or 4th residue from the carboxyl terminus. At the amino terminus of an ideal helix, the first three carbonyl groups are involved in hydrogen bonding, whereas the first three NH groups remain nonbonded. At the carboxyl terminus, the converse situation holds good, with the three NH groups hydrogen-bonded. Since proline cannot form a hydrogen bond, having this residue up to the third position at the carboxyl terminus is more detrimental to α-helical structure than having it at the amino terminus. Alternatively, the presence of a turn at the beginning could help stabilize a helix (Blagdon and Goodman, 1975).

The carboxyl-terminal SSSGEQE has also been shown to be important in toxin action (Shai *et al.*, 1988), with a 4000-fold decreased channel-forming ability of the 1–26-residue stretch of Pardaxin. The importance of charge at the entrance of a proteinaceous channel has been emphasized (Green and Anderson, 1991). It has, however, been established that the negative charges of SSSGEQE are not important for Pardaxin activity (Shai *et al.*, 1990). A transmembrane channel also requires optimized energy wells at the entrances of a channel (Anderson, 1989), and it is possible that SSSGEQE plays a structural role in the toxin's channel-forming abilities. The carboxyl-terminal SSSGEQE is random under all the conditions examined. This peptide is coupled to the LSAVGSAL fragment in the native toxin. The latter fragment also does not exhibit strong secondary structural propensities. The peptide KTLLSAVGSALSSSGEQE corresponding to carboxyl-terminal portion of the toxin has been shown to have weak helical propensities when examined by CD in TFE.[2] In the larger multihelix proteinaceous channels, it has been proposed that β-sheets or smaller helices may be present at the center of the helix cluster, hidden from the hydrophobic lipid tails (Lodish, 1988). Experimental evidence for such a motif has been obtained for a potassium channel (Yool and Schwarz, 1991). However, no such arrangement has been proposed or demonstrated for a bundle of helices formed by the aggregation of short independent peptides. The carboxyl-terminal SSSGEQE could conceivably be visualized in such a superstructure in the membrane although our circular dichroism and NMR studies (Zagorski *et al.*, 1991) indicate the absence of its adopting any secondary structure (in isolation or as part of the entire toxin). Thus, the reason for the important role of this heptapeptide in toxin action must await determination of the toxin structure in membranes.

Although the ellipticities of pardaxin in SDS micelles had been reported as $[\theta]_{208}$ and $[\theta]_{222} \sim -15{,}000$ degrees cm^2/dmol (Thompson *et al.*, 1986), circular dichroism studies of the toxin in other media have been reported only recently (Shai *et al.*, 1990). The spectrum in water ($[\theta]_{205} \sim -3{,}000$ degrees cm^2/dmol, $[\theta]_{222} \cong -6{,}000$ degrees cm^2/dmol, and crossover ~ 202 nm) is indicative of ~30% α-helix, 30% β-sheet, and 40% random coil (Greenfield and Fasman, 1969). The spectrum in MeOH, however, is characterized by a single minimum at ~220 nm ($[\theta]_{220} \cong -10{,}000$ degrees cm^2/dmol, crossover ~ 208 nm) indicating 60–80% β-sheet content. The spectrum in the presence of soybean lecithin vesicles is indicative of a mixture of α-helix and β-sheet, with a minimum at 222 nm ($[\theta]_{222} \cong -15{,}000$ degrees cm^2/dmol), a shoulder at 215 nm ($[\theta]_{215} \sim -12{,}000$ degrees cm^2/dmol), and a crossover ~ 205 nm. Although the authors have interpreted the activities of pardaxin and its analogs in terms of changes in α-helical content, the MeOH and lecithin vesicle spectra clearly indicate significant β-sheet content. Zagorski *et al.* (1991) have determined the structure of pardaxin in 1:1 trifluoroethanol:water, using two-dimensional NMR techniques. Based on the pattern of inter-residue NOE connectivities involving NH, $C^{\alpha}H$, $C^{\beta}H$, $C^{\gamma}H$, and $C^{\delta}H$ protons, they have identified 5 structurally distinct peptide segments: 1–5, 6–11, 12–13, 14–26, and 27–33. Segment 6–26 is proposed to have a helix-bend-helix conformation with the bend centered at residues 12 and 13. A random structure has been proposed for the carboxyl-terminal end (residues 27–33). Although the 1–5 region is not as ordered as the subsequent segments, the NMR data suggest the presence of some ordering of the side chains. However, the structure of pardaxin has not been determined in the membrane by high resolution techniques like NMR. While it is conceivable that the conformational behavior of the various segments of the toxin in solution may be of limited relevance to their structure in the toxin in the membrane, our results presented in this paper and the conclusions from the NMR study (Zagorski *et al.*, 1991) indicate that elements of secondary structure like helical conformations are present in short peptides that correspond to helical regions in the toxin in solution. Also, the carboxyl-terminal fragment SSSGEQE has no strong secondary structural propensities in isolation as well as when part of the entire toxin. Thus, amino-terminal and central regions are likely to have an important role in initiating and maintaining helical conformation of pardaxin. The investigations by Dyson *et al.* (1992) suggest that elements of secondary structure like reverse turns, nascent helix, and ordered helical conformation are abundant in short peptide fragments corresponding to helical regions of proteins. These structures are presumed to play an important role in folding of helical proteins. Our study suggests that short segments of amphipathic, membrane-active, helical peptides composed of 25–35 residues have strong propensities to occur in helical conformations, particularly in apolar solvents, and are likely to have an important role in initiating and maintaining helical conformation of the parent peptide.

Acknowledgment—We thank V. M. Dhople for amino acid analysis.

REFERENCES

Anderson, O. S. (1989) *Methods Enzymol.* **171,** 62–112
Andreu, D., Ubach, J., Boman, A., Wahlin, B., Wade, D., Merrifield, R. B., and Boman, H. G. (1992) *FEBS Lett.* **296,** 190–194
Blagdon, D. E., and Goodman, M. (1975) *Biopolymers* **14,** 241–245
Boman, H. G., Wade, D., Boman, I. A., Wahlin, B., and Merrifield, R. B. (1989) *FEBS Lett.* **259,** 103–106
Bruch, M. D., and Gierasch, L. M. (1990) *J. Biol. Chem.* **265,** 3851–3858
Chen, Y. H., Yang, J. T., and Chau, K. H. (1974) *Biochemistry* **13,** 3350–3359
Chou, P. Y., and Fasman, G. D. (1978) *Adv. Enzymol. Relat. Areas Mol. Biol.* **47,** 45–148
Dempsey, C. E. (1990) *Biochim. Biophys. Acta* **1031,** 143–161
Dyson, H. J., Merutka, G., Waltho, J. P., Lerner, R. A., and Wright, P. E. (1992) *J. Mol. Biol.* **226,** 795–817
Fox, R. O., and Richards, F. M. (1982) *Nature* **300,** 325–330
Green, W. N., and Anderson, O. S. (1991) *Annu. Rev. Physiol.* **53,** 341–359
Greenfield, N., and Fasman, G. D. (1969) *Biochemistry* **8,** 4108–4116
Hoyt, D. W., and Gierasch, L. M. (1991) *Biochemistry* **30,** 10155–10163
Kaiser, E. T., and Kezdy, F. J. (1987) *Annu. Rev. Biophys. Biophys. Chem.* **16,** 561–581
Keller, R. C. A., Killian, J. A., and de Kruijff, H. B. (1992) *Biochemistry* **31,** 1672–1677
Lee, K. H., Fitton, J. E., and Wüthrich, K. (1987) *Biochim. Biophys. Acta* **911,** 144–153
Lelkes, P. I., and Lazarovici, P. (1988) *FEBS Lett.* **230,** 131–136
Lodish, H. F. (1988) *Trends Biochem. Sci.* **13,** 332–334
Manning, M. C., Illangasekare, M., and Woody, R. W. (1988) *Biophys. Chem.* 77–86
Mattice, W. L., and Harrison, W. H. (1975) *Biopolymers* **14,** 2025–2033
Nagaraj, R., and Balaram, P. (1981a) *Accts. Chem. Res.* **14,** 356–362
Nagaraj, R., and Balaram, P. (1981b) *Biochemistry* **20,** 2828–2835

Nagaraj, R., and Balaram, P. (1981c) *Tetrahedron Lett.* **37,** 1263–1270
Nagaraj, R., Shamala, N., and Balaram, P. (1979) *J. Am. Chem. Soc.* **101,** 16–20
Padmanabhan, S., Marqusee, S., Ridgeway, T., Lave, T. M., and Baldwin, R. (1990) *Nature* **344,** 268–270
Pal, R., Barenholz, Y., and Wagner, R. R. (1981) *J. Biol. Chem.* **256,** 10209–10212
Primor, N. (1984) *Br. J. Pharmacol.* **82,** 43–49
Primor, N., and Lazarovici, P. (1981) *Toxicon* **19,** 573–578
Primor, N., and Tu, A. T. (1980) *Biochim. Biophys. Acta* **626,** 299–306
Primor, N., and Zlotkin, E. (1975) *Toxicon* **13,** 227–231
Primor, N., and Zlotkin, E. (1976) in *Animal, Plant and Microbial Toxins* (Ohsaka, A., Hayashi, K., and Sawai, Y., eds) Vol. 1, pp. 287–293, Plenum Publishing Corp., New York
Primor, N., Parness, J., and Zlotkin, E. (1978) *Animal, Plant and Microbial Toxins* (Ohsaka, A., Hayashi, K., and Sawai, Y., eds) pp. 287–291, Plenum Publishing Corp., New York
Primor, N., Sabnay, I., Lavie, V., and Zlotkin, (1980) *Eur. J. Exp. Zool.* **211,** 33–43
Primor, N., Zadunaisky, J. A., and Tu, A. T. (1983) in *Shark Repellents of the Sea: New Perspectives* (Zahuranec, B. J., ed) pp. 183–184, American Association for the Advancement of Science, Washington, D.C.
Primor, N., Zadunaisky, J. A., Murdaugh, M. V., Boyer, J. L., and Forrest, J. N. (1984) *Comp. Biochem. Physiol.* **78,** 484–490
Ramachandran, G. N., and Sasisekharan, V. (1968) *Adv. Protein Chem.* **23,** 238–283
Reddy, G. L., and Nagaraj, R. (1986) *Proc. Indian Acad. Sci. Chem. Sci.* **97,** 71–75
Reddy, G. L., and Nagaraj, R. (1989) *J. Biol. Chem.* **264,** 16591–16597
Reddy, G. L., Bikshapathy, E., and Nagaraj, R. (1985) *Tetrahedron Lett.* **26,** 4257–4260
Saberwal, G., and Nagaraj, R. (1989) *Biochim. Biophys. Acta* **984,** 360–364
Shai, Y., Fox, J., Caratsch, C., Shih, Y. L. Edwards, C., and Lazarovici, P. (1988) *FEBS Lett.* **242,** 161–166
Shai, Y., Bach, D., and Yanovsky, A. (1990) *J. Biol. Chem.* **265,** 20202–20209
Taylor, J. W., and Kaiser, E. T. (1987) *Methods Enzymol.* **154,** 473–498
Thompson, S. A., Tachibana, K., Nakanishi, K., and Kubota, I. (1986) *Science* **233,** 341–343
Toniolo, C., Bonora, G. M., Salardi, S., and Mutter, M. (1979) *Macromolecules* **12,** 620–625
Yool, A. J., and Schwarz, T. L. (1991) *Nature* **349,** 700–704
Zagorski, M. G., Norman, D. G., Barrow, C. J., Iwashita, T., Tachibana, K., and Patel, D. J. (1991) *Biochemistry* **30,** 8009–8017